CONFERENCES AND SYMPOSIA

PACS number: 01.10.Fv

Joint scientific session of the Physical Sciences Division of the Russian Academy of Sciences and the Joint Physical Society of the Russian Federation "Nonlinear acoustic diagnostics" (28 September 2005)

A joint scientific session of the Physical Sciences Division of the Russian Academy of Sciences (RAS) and the Joint Physical Society of the Russian Federation was held on September 28, 2005 in the Conference Hall of the Lebedev Physics Institute, RAS under the name "Nonlinear acoustic diagnostics." The following reports were presented at the session:

(1) **Rudenko O V** (Lomonosov Moscow State University) "Giant nonlinearities in structurally inhomogeneous media and the fundamentals of nonlinear acoustic diagnostics methods";

(2) **Zaitsev V Yu, Nazarov V E, Talanov V I** (Institute of Applied Physics, RAS, Nizhny Novgorod) "'Nonclassical' manifestations of microstructure-induced nonlinearities: new prospects for acoustic diagnostics";

(3) **Esipov I B, Rybak S A, Serebryanyi A N** (Andreev Acoustics Institute, RAS) "Nonlinear acoustic diagnostics of the ocean and rock";

(4) **Preobrazhenskii V L** (Research Center for Wave Studies, Prokhorov Institute of General Physics, RAS, European Laboratory in Nonlinear Magneto-acoustics (LEMAC)) "Parametrically phase-conjugate waves: applications in nonlinear acoustic imaging and diagnostics."

An expanded version of the report by Rudenko is published in the 'Physics of our days' section of this issue. An abridged version of reports 2 – 4 is given below.

PACS numbers: **43.25.+y**, 62.20.Mk, **62.65.+k**
DOI: 10.1070/PU2006v049n01ABEH005877

'Nonclassical' manifestations of microstructure-induced nonlinearities: new prospects for acoustic diagnostics

V Yu Zaitsev, V E Nazarov, V I Talanov

1. 'Classical' lattice nonlinearity and microstructure-induced acoustic nonlinearity

In solid-state physics, deviations from linear elasticity are traditionally attributed to a weak unharmonicity of the interatomic potential [1]. To describe such nonlinearity, it is usually sufficient to amend the linear term in Hooke's law by terms proportional to the square and cube of the deformation tensor, $\sigma = E\,(\varepsilon + \gamma^{(2)}\varepsilon^2 + \gamma^{(3)}\varepsilon^3 + \ldots)$, where σ is the elastic tension, ε is the deformation tensor, and E is the elastic modulus. For simplification, we limit our analysis to longitudinal deformations. For homogeneous amorphous materials and monocrystals, the dimensionless quadratic and cubic nonlinearity coefficients $\gamma^{(2)}$ and $\gamma^{(3)}$ are typically of the order of unity, whereas the deformations are usually quite small (for instance, $\varepsilon < 10^{-5}$ even for intense acoustic loads and $\varepsilon < 10^{-3}$ for 'usual' mechanical loads). Therefore, nonlinear corrections are usually very small in comparison with the linear term, but just these corrections are responsible for the well-known effects of thermal expansion and the dependence of the velocity of elastic waves on mechanical load and temperature. Based on such effects, the estimated nonlinearity coefficients are in good agreement with the conventionally adopted shape of the interatomic potential characterized by weak unharmonicity [1]. But the discrepancy of 2 to 4 orders of magnitude between the theoretical estimates of the breakdown threshold loads and the experimental data for the same potential was already found in the 1920s. The search for the reasons for this discrepancy has led to the understanding of the importance of microstructure imperfections and has significantly contributed to the formation of an important research field, the physics of dislocations.

Breakdown is an extreme form of materials' nonlinear behavior. Even though it is extremely sensitive to microstructure imperfections, it obviously cannot be used for diagnostic purposes. The amplitudes of deformations in the acoustic range are smaller than the breakdown deformations by several orders of magnitude; however, they already reveal microdefects by modified nonlinear properties of the medium. In the 1970s, the changes in metal microstructure due to accumulated fatigue-caused damage were first experimentally observed to result in a severalfold higher acoustic nonlinearity manifesting itself, for instance, in a significantly larger amplitude of higher harmonics of the probing acoustic wave [2 – 4]. Later, it was found that in contrast to the manifestations of the 'classical' power-law elastic nonlinearities, qualitative modifications of nonlinear effects may often occur, including functional modifications in amplitude dependences, the appearance of new nonlinear dissipative properties, and hysteresis. Data of this kind are available for many very different media, such as metals with fatigue- or heat-caused damage, rocks, many man-made materials (including composites) with crack-like imperfections, delaminations and inter-granular contacts [2 – 12], metal nanocrystals [13], and granular media [14].

From the standpoint of the possible use of nonlinear acoustic effects in diagnostics, it is especially important that

Uspekhi Fizicheskikh Nauk **176** (1) 97 – 112 (2006)
Translated by D V Belyaev; edited by A M Semikhatov

the high 'structural sensitivity' of the acoustic nonlinearity (concerning both its quantitative level and qualitative features) is often observed at the very first stage of damage of a material when its linear elastic moduli remain practically unchanged. Traditional linear methods, e.g., based on registering variations in the velocities of propagation of elastic waves or the equivalently changing fundamental frequencies cannot yet produce a definitive result at this stage of material damage.

2. Why is the variability of the nonlinear acoustic properties so great?

Due to the diversity of types of microstructural imperfections and to the broad range of media demonstrating anomalous acoustic nonlinearity both qualitatively and quantitatively, the mechanisms of its origin may also seem to be quite diverse, and specific physical models of nonlinear properties should therefore have predictive force only for rather limited classes of materials. On the other hand, alternative purely phenomenological, experiment-based stress – strain relations are more general, but do not allow relating the nonlinear properties of the medium to its microstructural features. Therefore, the models needed should reasonably compromise between the above-mentioned extreme cases and be useful for predictions.

The analysis of copious data by various groups on microstructure-induced acoustic nonlinearity (disregarding the exotic interactions of the acoustic mode with the other nonacoustic strongly nonlinear mode, which is coupled, for example, with the electron or spin subsystem) allows making the following fairly general statement. In most cases of microinhomogeneous media, a strong increase in acoustic nonlinearity of a material results from the presence of some structural features with strongly decreased rigidity, the sizes of these soft imperfections being small on the scale of the elastic wavelength, and their concentration being also small (in the sense specified below). Cracks are characteristic examples of such relatively soft imperfections. Various known models agree that a crack may be completely closed by the compressing load that produces a strain in the surrounding medium approximately equal to the ratio of the crack opening d to its diameter L. This actually means that a crack is approximately L/d times softer than the surrounding medium. The values of the d/L ratio are often quite low, $10^{-3}-10^{-5}$. Another characteristic example is intergrain contacts, which, due to their geometry (small contact area), are much more compressible than the grain bulk material. Aggregates of dislocations at grain boundaries in polycrystals are also significantly more compliant, first and foremost, to tangential loads, than the surrounding areas consisting of more homogeneous material.

Without specifying the types of imperfections, the features noted above can be described by a rather simple rheological model of a microinhomogeneous medium with soft contrasting imperfections [15, 16]. Even a one-dimensional variant of the model allows drawing some nontrivial conclusions. The model is based on the evident statement that nonlinearity (that is, the maximum deviations from Hooke's law) and increased dissipation are localized in the imperfections due to their high compressibility and, therefore, due to locally increased strain and the strain rate. The homogeneous medium that surrounds imperfections can be viewed here as a linearly elastic material that obeys Hooke's law, $\sigma = E\varepsilon$.

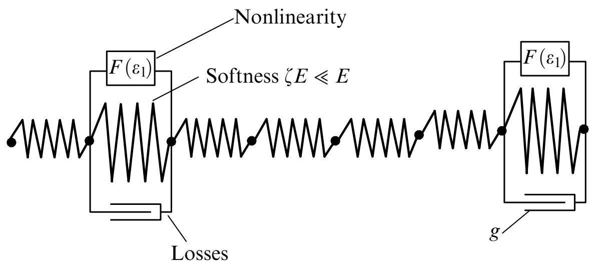

Figure 1. A rheological model of a medium with embedded contrasting soft defect inclusions at which nonlinearity and dissipation are localized.

This model of a microinhomogeneous medium is schematically given in Fig. 1. In this model, the most important parameters of imperfections are their compliance parameter (relative to the elastic modulus E of the matrix medium) given by a small parameter $\zeta \ll 1$, the concentration of soft imperfections v, that is, in the one-dimensional case, the linear concentration of soft imperfections, or, in the three-dimensional case, their relative volume. We consider the imperfection size to be much smaller than the elastic wave length, and the imperfections are considered to be viscoelastic and weakly nonlinear when the strain of the imperfections is measured on their own scale (we note that this local strain must be distinguished from the mean macroscopic strain). For each imperfection with the compliance parameter ζ, the equation of state taking the above properties into account is

$$\sigma = \zeta E\left[\varepsilon_1 + F(\varepsilon_1)\right] + g\,\frac{\mathrm{d}\varepsilon_1}{\mathrm{d}t}\,. \tag{1}$$

The parameter g describes the effective viscosity of imperfections and the function $F(\varepsilon_1)$ describes their nonlinearity. For instance, $F(\varepsilon_1) = \gamma\varepsilon_1^2$ for quadratically nonlinear defects. The parameter γ here characterizes the imperfection nonlinearity on the scale of its own deformation ε_1, the magnitude of γ being in the standard range of several units. Using this model of a microinhomogeneous medium, for a low concentration of identical defects, we obtain [16] the following relation between the macroscopic material strain and stress:

$$\begin{aligned}\sigma(\varepsilon) &= E\varepsilon - Ev\Omega\int_{-\infty}^{t}\varepsilon(\tau)\,\exp\left[-\zeta\Omega(t-\tau)\right]\mathrm{d}\tau\\ &\quad + vE\Omega\zeta\int_{-\infty}^{t}\exp\left[-\zeta\Omega(t-\tau)\right]\\ &\quad \times F\left\{\Omega\int_{-\infty}^{\tau}\varepsilon(\tau')\exp\left[-\zeta\Omega(\tau-\tau')\right]\mathrm{d}\tau'\right\}\mathrm{d}\tau\,. \end{aligned}\tag{2}$$

Here, the notation $\Omega = E/g$ is used, with $\zeta\Omega$ denoting the relaxation frequency of the defects. In the case of different defects, averaging over their properties, that is, over the distribution $v(\zeta, g)$, must also be included in this equation. The first term on the right-hand side of (2) comes from the linear matrix medium, the second term is from the dissipation and linear reduction of the elastic modulus due to imperfections, and the third nonlinear term accounts for the combined effects of nonlinear and relaxational properties of imperfections. This term demonstrates the essence of the 'contrast structural mechanism' of the nonlinearity increase due to locally strongly increased strain at the soft defects. This is especially clear in the quasistatic limit. In this case, for instance, for the defects characterizes by a power-type nonlinearity of the nth order, with $F(\varepsilon_1) = \gamma^{(n)}\varepsilon_1^{(n)}$, the macroscopic stress – strain relation takes the simple form

$$\sigma = \varepsilon E_{\text{eff}}\left(1 + \varepsilon^{n-1}\gamma_{\text{eff}}^{(n)}\right),$$

which is valid for $0 \leqslant v \leqslant 1$ [15], where

$$\frac{E_{\text{eff}}}{E} = \frac{1}{1 - v + v/\zeta}, \quad \frac{\gamma_{\text{eff}}^{(n)}}{\gamma^{(n)}} = \frac{1 - v + v/\zeta^n}{(1 - v + v/\zeta)^n}. \tag{3}$$

These relations imply (see Fig. 2) that the locally increased deformation at the soft defects (characterized by the compliance parameter $\zeta \ll 1$) predominantly manifests itself in the growth of the nonlinear terms in the equation of state rather than in the drop in the linear elastic modulus. For a given value of the compliance parameter ζ, there is a range of imperfection concentrations $v < \zeta \ll 1$ where the linear elastic modulus remains practically unchanged, whereas the material's nonlinear parameter already grows severalfold (see Fig. 2). In this range of low concentrations, linear methods are not sensitive enough to produce a definite result and the use of nonlinear effects is attractive for early detection of 'weak features,' primarily, the incipient of cracks in material. Interestingly, the dependence of the nonlinearity coefficients $\gamma_{\text{eff}}^{(n)}/\gamma^{(n)}$ of different orders on the concentration of imperfections v has a clear maximum $\gamma_{\text{eff}}^{(n)}/\gamma^{(n)} = [(n-1)/\zeta]^{n-1}/n^n \gg 1$. With the higher nonlinearity order, the maximum is reached at the lower imperfection concentration $v_{\text{opt}} \approx \zeta/(n-1) \ll 1$ and the maximum value is greater. This nonmonotonic nonlinearity growth is caused by the interplay between the locally increased deformations at the soft defects and their concentration (volume content). The analogous phenomenon is known in acoustics of gas – liquid mixtures exhibiting strongly increased nonlinearity due to the structural 'contrast mechanism,' whereas pure liquids and gases are classical weakly nonlinear media [17].

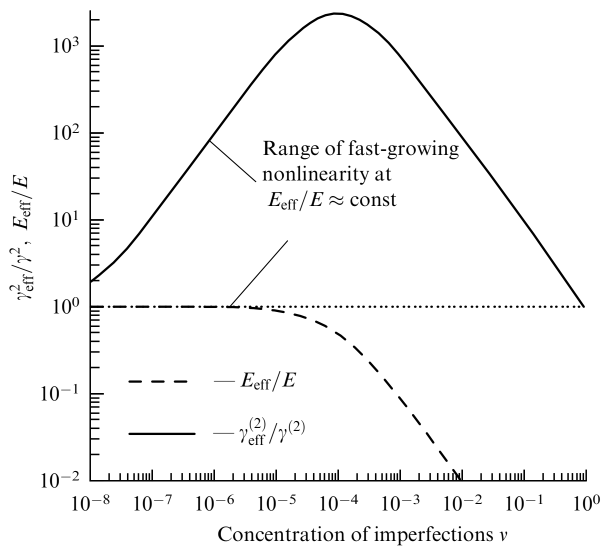

Figure 2. Complementary relative changes in the elastic modulus E_{eff}/E and in the quadratic nonlinearity parameter $\gamma_{\text{eff}}^{(2)}/\gamma^{(2)}$ for a microinhomogeneous medium containing defects with the relative compliance parameter $\zeta = 10^{-4}$, which is typical of cracks.

3. Qualitative 'nonclassical' features of the microstructure-induced nonlinearity

In the case of solids, the soft defects that we consider have some features, in addition to compliance itself, leading to unusual consequences. For example, microcontact-like and crack-like imperfections have both relaxational and specific nonlinear properties. In particular, the Hertz contacts have the fractional nonlinearity exponent 3/2 with respect to compression load and at the same time behave as diods, because they do not 'hold' a tensile load [14]. In addition, due to friction and adhesion, the same imperfections may result in stress – strain hysteresis of the material [5 – 7].

These features combined provide a wide diversity of 'nonclassical' manifestations of structure-induced nonlinearity. For example, even simplified Eqn (2) shows that for the quite common quadratic elastic nonlinearity $F(\varepsilon_1) = \gamma\varepsilon_1^2$ of the defects, their relaxational properties result in a pronounced frequency dependence of the effective nonlinear parameters, which is not typical of the classical lattice nonlinearity. Actually, a traditional intuitive approach, which accounts for nonlinearity and relaxation via additive terms, does not work for a microinhomogeneous medium. The additive approach becomes inapplicable because both nonlinear and relaxational properties of a microinhomogeneous medium are mainly localized in the same places, the soft imperfections. Thus, the relaxational 'freezing' of the response of imperfections to acoustic waves with frequencies greatly exceeding the relaxational frequency $\zeta\Omega$ simultaneously weakens their nonlinear response. For example, for the conventionally studied frequency mixing effect, the effective values of the quadratic nonlinear parameter may be considerably lower for the sum harmonics than for the difference-frequency harmonics.

Equation (2) also predicts another nontrivial manifestation of this contrast soft – rigid microheterogeneity of the medium: at moderate static and dynamic strains (e.g., $\varepsilon \sim 10^{-5}$, typical of acoustic waves), there is a possibility of a severalfold change in the acoustic dissipation in microinhomogeneous materials due to the combined action of the linear relaxational dissipation and the purely elastic nonlinearity $F(\varepsilon_1)$ [18]. It is important that at such strong changes in the dissipation, the complementary changes in the linear elasticity may still be very small, about 1%. Indeed, almost all dissipation in microinhomogeneous media is localized at soft defects such as cracks, which only weakly affect the macroscopic elastic modulus at small concentration. Therefore, even the complete closing of the cracks under compressing load may change the material elasticity merely insignificantly, whereas the *relative* change of dissipation may be arbitrarily large (from a finite value down to nearly zero). In a homogeneous medium, when the Kelvin – Voight or similar classical rheological visco-elastic models are applicable, such a drastic difference in variations of elasticity and dissipation is impossible.

The lack of space does not allow us to discuss these and other interesting consequences of the rheological model in more detail [15, 16]. We note that its implications are supported by the direct analysis of nonlinear and thermoelastic effects at Hertzian microcontacts in cracks [11, 12]. First, this analysis predicts a highly increased level of thermoelastic losses, up to 4 – 6 orders of magnitude larger than the estimates of the thermoelastic contribution to dissipation conventionally discussed in geophysics. Second, it explains the high sensitivity of these losses to quite moderate average deformation of the medium. Indeed, the internal dissipating contacts may be considerably disturbed at typical acoustic strains $\varepsilon \sim 10^{-7} - 10^{-5}$, which are much smaller than the mean strains $\varepsilon \sim 10^{-4} - 10^{-3}$ required for the complete closing/opening of cracks.

4. Experimental examples

One of the first impressive demonstrations of the high sensitivity of acoustic nonlinearity to microstructural imperfections was the application of this phenomenon to quality control of the adhesion bonding of the thermal-insulation tiles for the Soviet space shuttle 'Buran.' The method exploited the enhanced level of the second harmonic at the local vibrational excitation of the debonded area [19]. The standard ultrasonic defectoscopy cannot be applied there because of the too high absorption of ultrasound by the tile material.

In many cases, however, the modulation of a probe wave by another independently generated perturbation (including impact perturbations) is more convenient than the registration of higher harmonics. An example of using the modulation spectra to detect a single crack of several millimeters in size in a railroad wheel axle is given in Fig. 3. The probe ultrasonic wave was modulated by the impact-generated oscillations at eigenfrequencies of the samples.

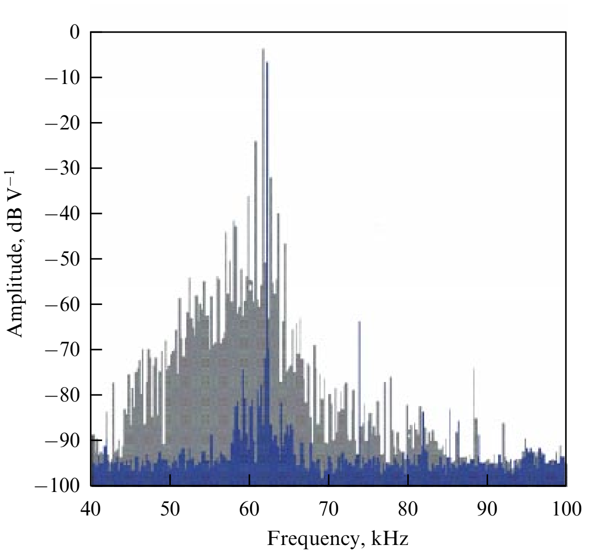

Figure 3. The diagnostics of microcracks in railroad wheel axles by nonlinear modulation. The modulation spectra of a defect-free axle and an axle with a single crack are drawn by the darker and by the lighter color, respectively. The modulation contrast is over 45 dB.

Unlike the absorption in homogeneous media, the absorption in microinhomogeneous media is pronouncedly amplitude-dependent. Together with the conventional modulation technique, this amplitude-dependent dissipation allows using the effect of amplitude modulation transfer from a carrier wave ('pump') to another initially nonmodulated probe wave for the purposes of diagnostics. This acoustic effect is a direct analog of the so-called Luxemburg – Gorky effect of cross-modulation of radio waves in ionosphere. Figure 4 shows an example of using the acoustical cross-modulation technique to monitor structural rearrangements in a grainy medium subjected to weak artificial 'seismic events' in laboratory conditions [21]. In the experiment, the amplitude modulation (30 Hz) was transferred from the carrier 'pump' wave (7 kHz) to a probe wave (10 kHz).

Successful field observations of the probe seismic wave modulation under the action of another deformation field [22, 23] and seismic-wave self-action [24] at amplitudes that are typical of the existing seismic sources [22 – 25] suggest that the

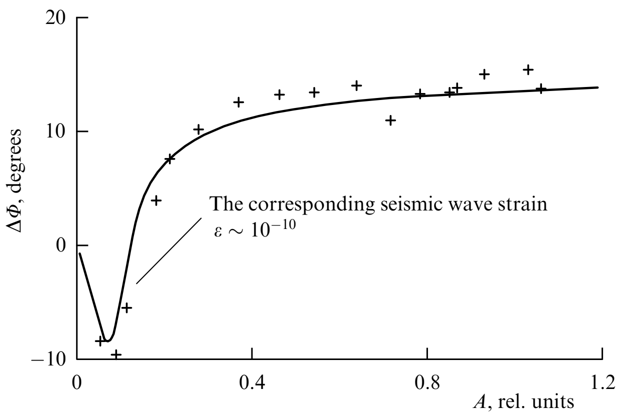

Figure 5. Nonlinear phase shift versus amplitude for a seismic wave of an extremely low amplitude radiated by a highly coherent source with the frequency 230 Hz. Crosses are the experimental data and the curve is theoretical simulation [24].

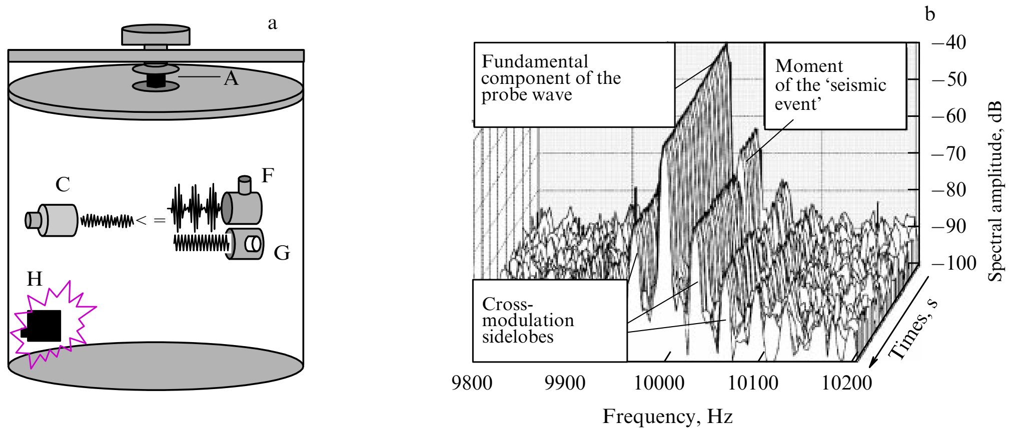

Figure 4. (a) Sketch of the experimental setup for observation of the acoustic analog of the Luxemburg – Gorky effect: A — force cell, C — receiver, F and G — sources of the pump and probe waves, H — shaker. (b) An example of strong (10 – 15 dB) variations of pump-induced cross-modulation sidelobes of the probe wave in an artificial granular medium. The variations in the probe wave amplitude at the fundamental frequency were hardly noticeable [21].

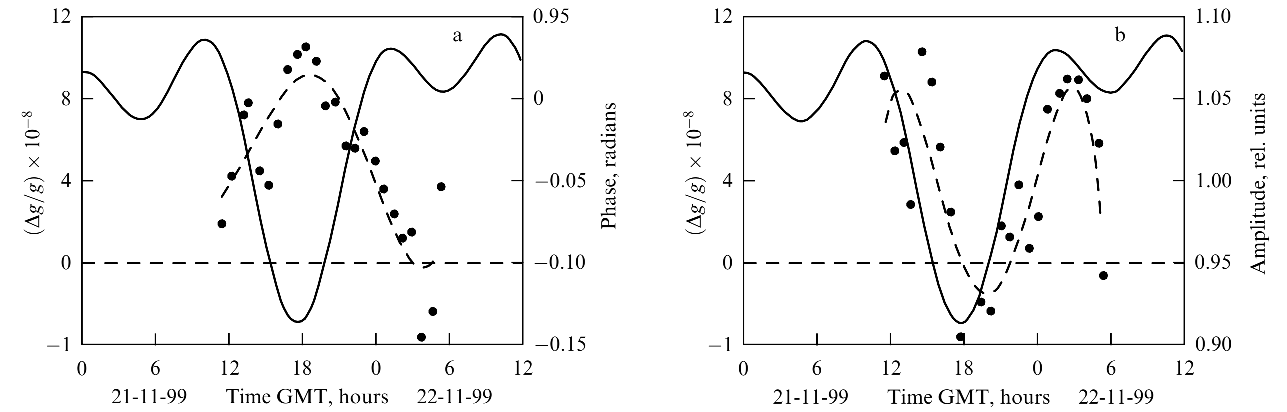

Figure 6. Tidal variations of the amplitude (a) and the phase (b) of a seismic wave with the frequency 167 Hz propagating in gas- and oil-saturated sandstone over the distance 360 m. The dashed lines fit the experimental points and the solid lines represent tidal variations in the local gravitational acceleration [23].

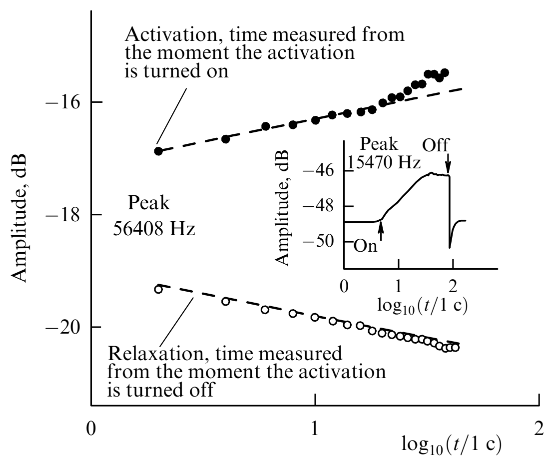

Figure 7. An example of slow dynamics of amplitudes (quality factors) of two probe-wave resonances in a steel sample with a single crack during acoustic 'loading' of it by another wave and during the relaxation after it is turned off. The solid circles and white circles represent the activation and the relaxation stages with the time measured from the moments the loading wave turned on and off, respectively. In the inset, the time scale is continuous, and the time points when the loading wave is turned on and off are shown by arrows.

nonlinear technique can be useful not only in nondestructive testing but also in seismic monitoring (at least at seismic-engineering scales of several hundred meters). Figure 5 presents an example of the seismic wave phase shift as a function of the excitation amplitude for the propagation distance 120 m in sandy sediments [24]. Another example of a field seismic experiment [23] is given in Fig. 6. Here, a seismic wave from a powerful down-hole source [25] exhibits amplitude and phase modulation by the field of tidal deformations.

Other examples of 'nonclassical' manifestations of micro-structure-induced nonlinearity include a time-reversible effect of slow thermoelastic dynamics recently found to occur for cracks, combined slow and 'instant' nonlinear effects, the use of nonlinear acoustics for evaluation of the distribution of contact forces in granular media in the previously inaccessible range of very weak forces much below the average value, and other effects [11, 12, 14, 21, 26]. We limit ourselves here to an example (Fig. 7) of the logarithmic-in-time, reversible, and velocity-symmetric slow thermoelastic dynamics observed for a single crack [12, 26].

The results given here and similar data by other authors suggest a wide diversity of applications of nonlinear acoustic effects in material science, nondestructive testing, and seismic monitoring, which explains the worldwide growing attention to these studies.

In conclusion, we note that this brief review of the research conducted at the Institute of Applied Physics, RAS was to a large extent motivated by the pioneering works on nonlinear acoustics done since the 1960s – 1970s under the direction of V A Zverev and L A Ostrovskii.

The results presented were obtained with the partial support of the Russian Foundation for Basic Research (grants No. 05-05-64941 and 05-02-17355), the Ministry of Industry and Science, the program "Coherent acoustic fields and signals" of the Physics Division of RAS (grant No. NSh — 1641.2003.02), and the joint program of the Russian Academy of Sciences and Centre National de la Recherche Scientifique, France (project PECO — NEI No. 16366).

References

1. Kittel Ch *Introduction to Solid State Physics* (New York: Wiley, 1976) [Translated into Russian (Moscow: Nauka, 1978)]
2. Gedroits A A, Zarembo L K, Krasil'nikov V A *Dokl. Akad. Nauk SSSR* **150** 515 (1963) [*Sov. Phys. Dokl.* **8** 478 (1963)]
3. Gits I D, Gushchin V V, Konyukhov B A *Akust. Zh.* **19** 335 (1973)
4. Buck R O, Morris W L, Richardson J M *Appl. Phys. Lett.* **33** 371 (1978)
5. Nazarov V E et al. *Phys. Earth Planet. Inter.* **50** 65 (1988)
6. Nazarov V E *Akust Zh.* **37** 150 (1991) [*Sov. Phys. Acoust.* **37** 75 (1991)]
7. Guyer R A, Johnson P A *Phys. Today* **52** (4) 30 (1999)
8. Nazarov V E, Kolpakov A B *J. Acoust. Soc. Am.* **107** 1915 (2000)
9. Van Den Abeele K E-A *NDT&E Int.* **34** 239 (2001)
10. Ostrovsky L A, Johnson P A *Riv. Nuovo Cimento* **24** (7) 1 (2001)
11. Zaitsev V, Gusev V, Castagnede B *Phys. Rev. Lett.* **89** 105502 (2002)
12. Zaitsev V, Gusev V, Castagnede B *Phys. Rev. Lett.* **90** 075501 (2003)
13. Lang M J et al. *Nanostruct. Mater.* **12** 811 (1999)
14. Tournat V et al. *Phys. Rev. Lett.* **92** 085502 (2004)
15. Zaitsev V Yu *Acoust. Lett.* **19** 171 (1996)
16. Zaĭtsev V Yu, Nazarov V E, Belyaeva I Yu *Akust. Zh.* **47** 220 (2001) [*Acoust. Phys.* **47** 178 (2001)]
17. Rudenko O V, Soluyan S I *Teoreticheskie Osnovy Nelineinoi Akustiki* (Theoretical Foundations of Nonlinear Acoustics) (Mos-

cow: Nauka, 1975) [Translated into English (New York: Consultants Bureau, 1977)]
18. Zaitsev V, Sas P *Acta Acust. Acust.* **86** 429 (2000)
19. Antonets V A, Donskoi D M, Sutin A M *Mekhanika Komposit. Mater.* (5) 934 (1986)
20. Matveev A L et al. *V Mire Nerazrush. Kontr.* (4(26)) 65 (2004)
21. Zaitsev V Yu et al. *Europhys. Lett.* **70** 607 (2005)
22. Bagmet A L et al. *Dokl. Ross. Akad. Nauk* **346** 390 (1996) [*Dokl. Earth Sci.* **346** 135 (1996)]
23. Bogolyubov B N et al. *Geol. Geofiz.* **45** 1045 (2004)
24. Zaitsev V Yu, Nazarov V E, Talanov V I *Akust. Zh.* **45** 799 (1999) [*Acoust Phys.* **45** 720 (1999)]
25. Averbakh V S et al. *Akust. Zh.* **51** (dop. vyp.) 31 (2005) [*Acoust Phys.* **51** (Suppl.) 23 (2005)]
26. Zaitsev V, Nazarov V, Gusev V, Castagnede B *NDT&E Int.* (2005) (in press)

PACS numbers:: **43.25.+y**, 43.30.Pc, 83.80.Fg, **92.10.–c**
DOI: 10.1070/PU2006v049n01ABEH005878

Nonlinear acoustic diagnostics of the ocean and rock

I B Esipov, S A Rybak, A N Serebryanyi

1. Introduction

In the 1940s and 1950s, Russian studies on nonlinear acoustics were stimulated by the pioneering work of N N Andreev. His article 'On some second-order values in acoustics' was published in the first volume of *Akusticheskii Zhurnal* issued in 1955 [1]. In the 1960s, it was followed by the technological and medical applications of powerful ultrasound introduced by L D Rosenberg [2]. It was then that L M Brekhovskikh formulated the problem of the interaction between acoustic and oceanic waves [3]. Many Russian research groups worked in these areas. Recently, experts in propagation and interactions of nonlinear waves have started to address waves in granular media and continental shelf internal waves because both are essentially nonlinear. In granular media, the nonlinearity parameter is 3 – 4 orders of magnitude greater than that in homogeneous media, and the 'giant nonlinearity' term has been coined [4, 5]. Due to the high amplitudes and slow velocities, internal waves undergo essential nonlinear transformations.

In this report, the results of experimental observations of new nonlinear wave processes in the ocean and granular rocks are given.

2. Granular media

Acoustic waves are known to propagate in granular and in solid media differently. The mechanical properties of granular media are largely determined by the inter-granular contacts. This property allows assigning granular media to a broad class of media with nonlinear structural elasticity. Whereas the nonlinear acoustic properties of monocrystals, homogeneous fluids, and other solid media are determined by the molecular nature of their strain, the properties of granular media are determined by their structure. In this sense, the properties of granular media are seen at the mesoscale, that is, the scale of the granules [4]. This results in considerable qualitative and quantitative differences, including differences in the equations of state for the media. For a solid medium, the relative strain $\varDelta$ is assumed to be proportional to the stress applied, $\varDelta \approx P$, but the relation for the spherical granule is $\varDelta \approx P^{2/3}$ [6]. In granular media, the velocity of acoustic waves is therefore $c = (\partial P/\partial \rho)^{1/2} \approx P^{1/6}$, which is a nonlinear function of the stress P applied. In agreement with this, the nonlinearity parameter $\alpha = \rho_0 \partial c^2/\partial P \approx P^{-5/6}$ is also dependent on the stress applied. (Here, ρ is the medium density and ρ_0 is its value at equilibrium.) The nonlinear properties of granular media prove noticeable even at quite moderate strain. In rocks, for instance, nonlinear distortions are already observed at a strain equal to $\varDelta \approx 10^{-9}$ [4]. This strain range is typical even for quite moderate acoustic perturbations.

The behavior of granular media is currently being studied at the single-granule level [7 – 11]. Under low stress, the stress – strain relations are noticed to measurably deviate from regular relations. As a rule, the latter work only asymptotically under high enough stress, when the granular medium may be considered well-packed. Such media usually respond to repeated stress with stress – strain hysteresis. This property of granular media leads to a nonlinear distortion of acoustic waves with the second harmonic proportional to the squared signal amplitude and possibly exceeding the third harmonic. Oscillations of a single granule in a constant acoustic field are shown to slowly fluctuate [7].

We discuss the results of the experimental analysis of slow fluctuations of the nonlinear oscillations of the granule in a medium where the acoustic field is propagating. One-two Granite bits of the size 1 to 2 cm served as the granular medium in our experiments. The sound was produced by a piezoceramic plate and the detection was done by accelerometers mounted among the granules. The experimental setup is detailed in [12]. We note that the accelerometers were of the size scale of the granules.

The detected signal versus the intensity of sound produced is plotted in Fig. 1. In this and subsequent experiments, the frequency of the produced sound was 5.6 kHz. The signal was detected by two accelerometers positioned equidistantly from the sound source and separately from each other. The common character of response measured by both detectors can be seen. A linear relation between the sound intensity and the signal holds only on average, for a large range of signal amplitude variations. The response is different for the different detectors, pointing to the independent propagation

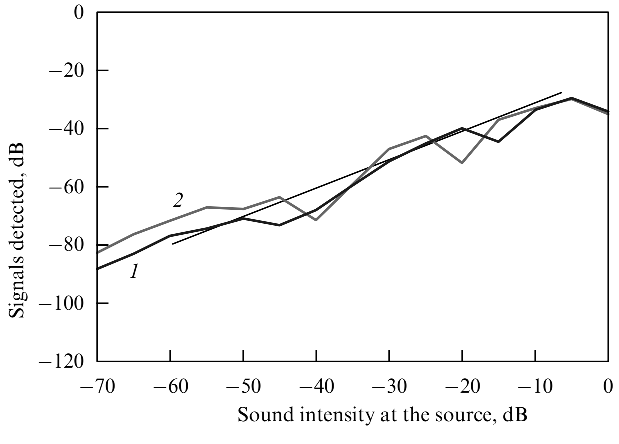

Figure 1. Signals detected in the granular medium versus sound intensity. The straight line corresponds to the linear response. Curves *1* and *2* are from different detectors.

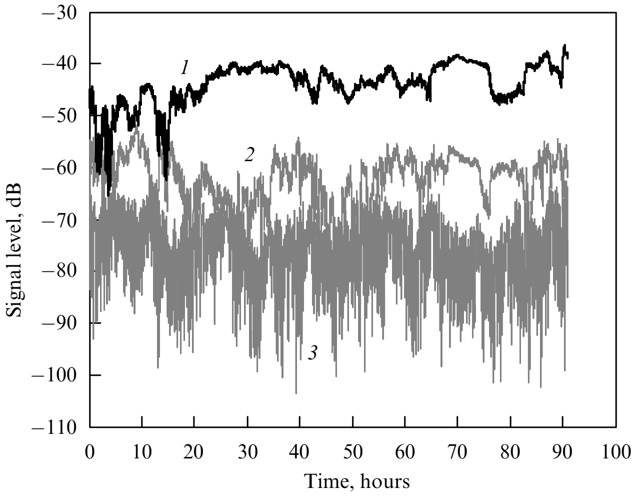

Figure 2. Time dependences of the harmonics of the signal detected in a granular medium: *1* — frequency 5.6 kHz, *2* — the second harmonic at 11.2 kHz, *3* — the subharmonic at 2.8 kHz.

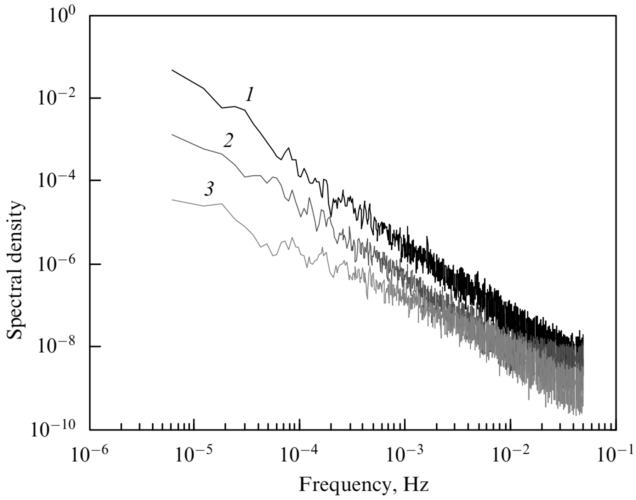

Figure 3. Fluctuation spectrum of spectral components of the signal in a granular medium. The signal level is 10 dB, *1* — frequency 5.6 kHz, *2* — frequency 11.2 kHz, *3* — frequency 2.8 kHz.

of the signal from the source to each detector. The maximum signal received corresponds to the source piezoceramic plate vibration with the acceleration 0.6 m c^{-2} and the amplitude equal to a mere 5 Å. These parameters correspond to a -10 dB sound level. The detected level of the granules' oscillations proved to be approximately 10dB lower. The nonmonotonic response of single granules to the stress applied to the medium is considered the result of percolate development of bonding of granules involved in transduction of the elastic signal from the source to the detector [13]. Such a percolate chain of inter-granule contacts is very sensitive to the stress parameters. A rise in stress leads to the chain restructuring and results in changes to its effective elasticity.

The results of the measurements of the acoustic field in the medium over time is given below. The signal at one of the detectors is given in Fig. 2 as a function of time, together with levels of the harmonics of the signal. First of all, we note that a subharmonic has appeared in the signal. The fluctuations of harmonics of the signals from both detectors are similar. The signal with the carrier frequency 5.6 kHz randomly changes by more than 5–6 dB. At the same time, the harmonics fluctuate much stronger, indicating the giant fluctuations of acoustic signals in granular media. The subharmonics fluctuates most intensely, as much as several tenfold.

The frequency spectra of the fluctuations of the signal harmonics are given in Fig. 3. The measurements were averaged over 32 realizations. The spectral analysis shows that random oscillations of low frequencies are the strongest fluctuations. Their frequencies are in the range $f = 10^{-5} - 10^{-1}$ Hz and monotonically drop with the frequency as $S(f) \approx Af^{-n}$. The exponent n proves to be different for different harmonics. It varies from $n = 2$ for the fundamental frequency 5.6 kHz to $n = 1.3$ for the subharmonics and always remains greater than one. Interestingly, at low frequencies, the exponent for the relation describing the spectrum of fluctuation frequencies happened to be near the values $n = 1.7 - 2.2$ measured in an experiment involving passing an acoustic signal through a medium composed of identical glass beads [7]. This points to a common mechanism of the low-frequency modulation of sound passing through media composed of granules of different shapes and sizes. The spectrum of fluctuations of the sound recorded must obviously reach a maximum or at least saturation at low frequencies when $n > 1$, because the intensity of fluctuations must remain finite. Our several-day-long experiments could not confirm this statement.

The experimental data involving registration of acoustic waves in granular media by granule-sized detectors point to the statistical nature of the process. In these conditions, a detector has a limited number of contacts with the adjacent granules and can be regarded as one of the elements of the medium. Even low constant amplitudes of sound in a medium result in great acoustic field fluctuations and in harmonics and subharmonics produced in it. The nonmonotonic dependence of the field in the medium on the sound amplitude points to a considerable role played by the inter-granular contacts in the formation of the acoustic field in a granular medium. In this case, acoustic perturbations are transmitted between granules via contacts only, which occupy a very small part of the granules and cannot therefore stabilize the medium. Thus, a granular medium may be considered to be in a metastable state and even a low-amplitude acoustic field may change the structure of its contacts. Such contacts form a structure of chains transmitting signals from the source to a detector. The density of such elastic chains is determined by the granule sizes and the number of inter-granular contacts. Acoustic oscillations shift inter-granular contacts slightly, possibly radically changing the structure of elastic chains and, therefore, the effective elastic properties of the medium. The acoustic impedance of the medium then also changes. During the contraction of a medium, the number of inter-granular contacts grows, resulting in a higher density of the elastic chains that transmit acoustic perturbations. The elastic properties of the medium then tend to saturation.

A possible mechanism of slow changes in the structure of contacts discussed in [7] is the thermal strain at the contact points of granules where acoustic energy is concentrated. The stable frequency response over the range $10^{-6} - 10^{-1}$ Hz may be due to the fractal structure of the elastic chains transmitting signals from the source to the detector.

To induce the subharmonics of an acoustic signal, quite intense acoustic fields are required. This phenomenon is usually observed during phase transitions. For a granular medium with elasticity determined by inter-granular contacts, the threshold amplitude for the phase transition is the specific gravity g. This value determines when a consolidated medium becomes nonconsolidated. The subharmonics appearing even at quite low signal amplitudes of 0.5 m c^{-2} point to the localization of the elastic energy of acoustic oscillations at separate granules of a granular medium.

Thus, the data obtained point to the complex character of the propagation of acoustic signals in granular media. The analysis of an acoustic field on the scale of a single granule has revealed the statistical nature of the process and its strong nonlinearity even at moderate amplitudes of the signal. The obtained experimental data allow developing a model for slow fluctuations of the acoustic field in granular media.

The acoustic diagnostics of granular media also have other features. The granular and other heterogeneous media belong to the class of acoustically dispersed nonlinear media. The combination of the nonlinearity and the dispersion allows obtaining soliton solutions for acoustic waves in such media. In particular, we derived the following equations for waves with resonance dispersion (RDE):

$$\left(\frac{\partial^2}{\partial t^2}+\omega_0^2\right)\left(\Delta U-\frac{1}{c^2}\,\frac{\partial^2}{\partial t^2}\,U+\alpha\Delta(U^2)+\Gamma\Delta\,\frac{\partial}{\partial t}\,U\right)$$
$$-\,\sigma^2\,\frac{\partial^2}{\partial t^2}\,U=0\,,$$

where α is the media nonlinearity, Γ is the dissipation, and σ^2 is the dispersion, which is proportional to the concentration of the oscillators in the medium [14, 15]. The solutions of this equation shown in Fig. 4 are specially shaped solitary solitons with vertical fronts. These solutions are quite sensitive to changes to the parameters of the medium such as dispersion, nonlinearity, and absorbance. Thus, following the shapes of such wave perturbations allows monitoring the state of media with resonance dispersion.

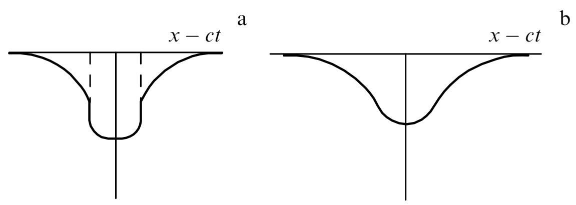

Figure. 4. A soliton of the wave equation with resonance dispersion: (a) medium without damping, (b) medium with damping.

3. Nonlinear acoustic processes in the ocean

We consider the capabilities of acoustic diagnostics of the ocean with the observations of internal waves taken as an example. Internal gravitational waves are frequent in the ocean and in the atmosphere. They exist because of the vertically stable stratification of the density of the medium. Any perturbation of such a medium leads to waves in it because the particles of the vertical column shifted from the equilibrium tend to return to their initial position under the action of the Archimedean force. A number of natural phenomena can produce this 'first push.' The most effective sources include tides, atmospheric perturbations, and ocean currents. The numerous sources of internal waves are so effective that, according to the well-known oceanologist W Munk, "no researcher of internal waves has yet reported calm at the depths of the ocean" [16]. Thus, internal waves are ubiquitous in the ocean; they create vertical water movements and facilitate the internal mixing necessary for life in the ocean. The characteristic parameters of internal waves are as follows: the periods vary from several days to several minutes and the wave speeds vary from several decimeters to several meters per second. The distribution of frequencies of the ocean internal waves drops proportionally to the frequency squared and has two peaks corresponding to long and short waves. The peak at long waves is from inertial and tidal waves, and the peak at short waves corresponds to the buoyancy frequency [17, 18]. The internal waves may be as high as several meters. In some regions of the ocean, giant internal waves higher than 100 m have been registered [19–22]. The internal waves come in series in space and time and propagate in a specific direction. In addition, solitary waves are observed. Internal-wave solitons are a widespread phenomena. Internal waves are typical for both the deep sea and the shelf. The shelf is where the internal waves are produced and simultaneously broken down with the energy of long waves transferred to short waves and further into turbulence. Here, the nonlinearity of the internal waves is seen most clearly [23, 24].

In recent years, we have analyzed internal waves of the Sea of Japan shelf by a multi-beam pulse sonar. We used the Acoustic Doppler Current Profiler (ADCP) Rio Grande 600 kHz from RD Instruments. Besides measuring a vertical and two horizontal components of the current, this instrument provides the data on reflection of the signal and locates the water density jump interfaces (pycnoclines) along which the propagating internal waves are seen. For the measurements, a small research boat was anchored for 24 hours or tacking at sea.

The research conducted has revealed the general picture of the internal wave dynamics and allowed more accurate measurements of their main parameters. During the measurements, a number of nonlinear effects fundamental for internal waves were confirmed. These effects were previously independently observed at other continental shelves by contact methods. Such effects include, first of all, the 'vertical' and the 'horizontal' asymmetry of the internal waves profile and the 'effect of changing the polarity of internal waves.'

The vertical asymmetry of crests and troughs. Intense internal waves propagating at a pycnocline (a layer with a density jump) that is closer to the bottom than to the sea surface have a characteristic profile with smooth feet and sharp crests and are therefore waves of elevation. In the case where the internal waves propagate at the thermocline that is closer to the surface than to the bottom, the wave profiles are characterized by smooth crests and sharp troughs and are therefore waves of depression. We often saw waves of elevation and waves of depression. Given in Fig. 5a is the record of a backscattered signal reflected from the deep water that was recorded in October of 2003 during passage through the Peter the Great Gulf in the Sea of Japan in the direction transverse to the coastline. Seen at the cross section obtained is the area of the subsurface pycnocline from the range 15–25 m, over which the solitary 5–10 m high waves of depression propagate. The internal waves propagate in the direction of the coast toward more shallow water. Given in Fig. 5b is the similar record taken in September of 2005 at the inner shelf when the density jump was near the bottom. In this case, a series of the internal waves of elevation with rank-ordered amplitudes up to 7 m propagates along the pycnocline toward the coast.

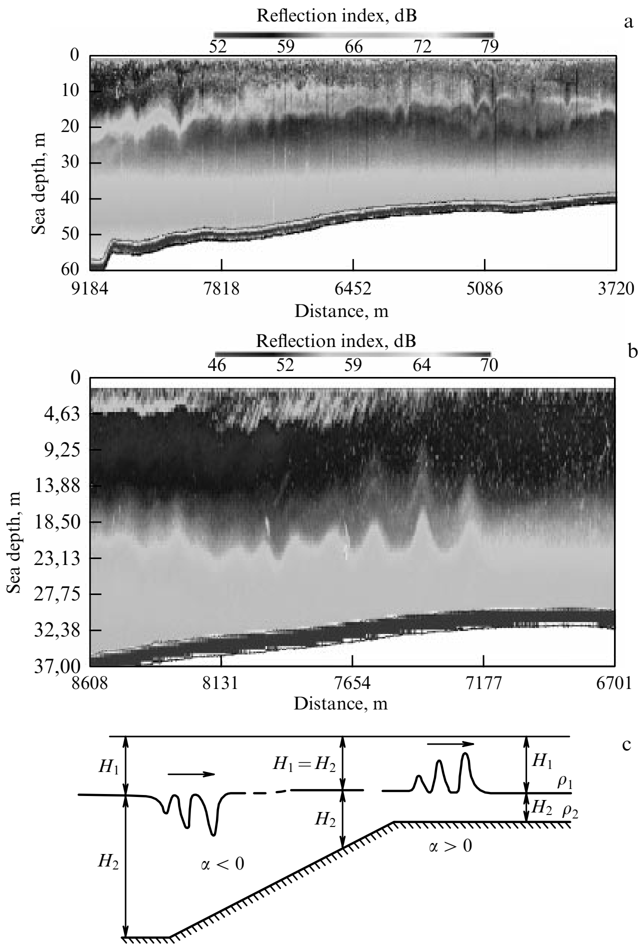

Figure 5. The vertical asymmetry of internal waves at a shelf. At the ocean cross sections of the refraction indices produced by the ADCP, the waves of depression (a) and the waves of elevation (b) are seen. (c) The explanation of the effect of changing the polarity of internal waves at a shelf; H_1 is the depth of the pycnocline, and H_2 is the depth from the pycnocline to the bottom.

The properties of vertically asymmetric internal waves at the shelf are close to those of solitons [24], and we can say that soliton-like waves of different polarities propagate at the shelf. This feature of internal waves at shelves results in an interesting phenomenon that we call the 'effect of changing the polarity of internal waves.' During the summer, the pycnocline at the near-coast part of the shelf is usually near the sea bottom, while at the deep sea part of the shelf, it is closer to the sea surface. Because soliton-like internal waves form at the shelf mainly from long tidal waves coming from the open sea and propagate toward the coast, they must switch from the near-surface pycnocline to the near-bottom pycnocline. At this point, the negative solitons (with negative nonlinearity) switch to the zone with the positive nonlinearity, and the waves of depression break down and become waves of elevation (Fig. 5c). At this point, the pycnocline is in mid-depth, and we call it the 'overturning point.' The first experimental proof of this effect came from observations at the Sea of Japan shelf [25, 23, 27] and was later confirmed by results from the Mediterranean Sea [26]. Recently, the best experiment under natural conditions was conducted in the South China Sea [28]. A high-frequency multi-beam acoustic sonar was used there as well. The transformation of the negative solitons of the internal waves at the switching point was numerically modeled [29]. The results of a special experiment studying the effect of changing the polarity of internal waves recently conducted by us at the Sea of Japan shelf are being prepared for publication.

The horizontal asymmetry of internal waves. The vertical asymmetry of internal waves discussed above is the main indicator of their nonlinearity. However, many intense internal waves are not only vertically but also horizontally asymmetric due to different inclinations of the front and the back slopes of the internal wave. This difference is a feature of a nonstationary wave, that is, a wave that is being destroyed. We repeatedly saw the horizontal asymmetry of internal waves during the measurements by the contact volume temperature sensors. The profiles of two internal waves of elevation propagating toward the coast are shown in Fig. 6. The recording in Fig. 6a was taken on October 1, 1982 at a sea depth of 30 m by the line temperature sensors and in Fig. 6b is the ADCP recording done on September 17, 2004 at a sea depth of 43 m. Both waves are about 10 m high, but their front slopes are considerably steeper than the back slopes. The recording from the contact volume temperature sensors is shown for two sensors situated at different distances from the coast: as the wave approaches the coast, it becomes steeper. The horizontal symmetry is very common for both elevation and depression intense internal waves at the shelves [30].

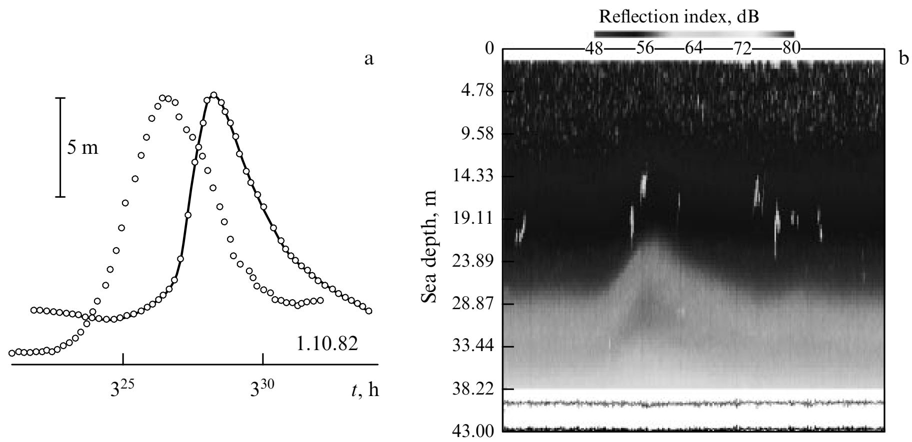

Figure 6. The horizontal asymmetry of internal waves measured by line temperature sensors (a) and by ADCP (b).

4. Conclusion

The considered examples of the acoustic diagnostics of nonlinear waves demonstrate new physical phenomena in granular rocks and the ocean. The metastable state of the granular media is an important condition for studies of acoustic effects on percolation in rocks. The nonlinear interaction of internal waves determines the transformation of the tidal energy into oceanic turbulence. The acoustic diagnostics prove to be effective for studying the dynamics of processes at the continental shelf.

This work was supported by the Russian Foundation for Basic Research (Gronts 05-02-17500, 05-02-16086, and 05-02-17406), by the INTAS Frant No. 04 80 7043, by the Program of Scientific School Support (grant NSh-1176.2003.2), by the Federal Targeted Program 'The World's Ocean' and by the company 'RD-Instruments-Europe'.

References

1. Andreev N N *Akust. Zh.* **1** 3 (1955)
2. Rozenberg L D (Ed.) *Fizika i Tekhnika Moshchnogo Ultrazvuka* Vol. 1 – 3 (Physics and Techniques of the Powerful Ultrasound) (Moscow: Nauka, 1967, 1968, 1970)
3. Brekhovskikh L M *Izv. Akad. Nauk SSSR Ser. Fiz. Atm. Okeana* **2** 970 (1966)
4. Ostrovsky L A, Johnson P A *Riv. Nuovo Cimento 2***4** (7) 1 (2001)
5. Rudenko O V *Usp. Fiz. Nauk* **176** 77 (2006) [*Phys. Usp.* **49** 69 (2006)]
6. Belyaeva I Yu, Zaitsev V Yu, Ostrovskii L A *Akust. Zh.* **39** 25 (1993)
7. Liu C, Nagel S R *Phys. Rev. Lett.* **68** 2301 (1992)
8. Liu C et al. *Science* **269** 513 (1995)
9. Miller B, O'Hern C, Behringer R P *Phys. Rev. Lett.* **77** 3110 (1996)
10. Herrmann H J, Stauffer D, Roux S *Europhys. Lett.* **3** 265 (1987)
11. Rintoul M D, Torquato S *Phys. Rev. Lett.* **77** 4198 (1996)
12. Bazhenova E D, Vil'man A N, Esipov I B *Akust. Zh.* **51** (Prilozhenie) 46 (2005) [*Acoust. Phys.* **51** (Suppl. 1) 37 (2005)]
13. Hidalgo R C et al. *Phys. Rev. Lett.* **89** 205501 (2002)
14. Rybak S A, Skrynnikov Yu I, in *Proc. of the IV Intern. Workshop "Nonlinear Waves in Resonant Dispersion Media"* (Singapore: Nonlinear World, 1989) p. 664
15. Rybak S A *Akust. Zh.* **44** 709 (1998) [*Acoust Phys.* **44** 617 (1998)]
16. Munk W, in *Evolution of Physical Oceanography: Scientific Surveys in Honor of Henri Stommel* (Eds B A Warren, C Wunsch) (Cambridge, Mass.: MIT Press, 1981) p. 264
17. Garrett C, Munk W *Geophys. Fluid Dynam.* **3** 225 (1972)
18. Konyaev K V, Sabinin K D *Volny Vnutri Okeana* (Waves Inside the Ocean) (St. Petersburg: Gidrometeoizdat, 1992)
19. Serebryany A N, in *Proc. of the 1st Intern. Symp. on Ocean Cities 95, Monaco, 20 – 23 November, 1995*, p. 376
20. Konyaev K V, Sabinin K D, Serebryany A N *Deep-Sea Res. I* **42** 2075 (1995)
21. Duda T F et al. *IEEE J. Ocean. Eng.* **29** 1105 (2004)
22. Sabinin K, Serebryany A *J. Marine Res.* **63** 227 (2005)
23. Serebryanyi A N *Izv. Akad. Nauk SSSR Ser. Fiz. Atm. Okeana* **26** 285 (1990)
24. Serebryanyi A N *Izv. Akad. Nauk SSSR Ser. Fiz. Atm. Okeana* **29** 244 (1993)
25. Serebryanyi A N *Okeanologiya* **25** 744 (1985)
26. Salusti E, Lascaratos A, Nittis K *Ocean. Modelling* **82** 10 (1989)
27. Serebryany A N, in *Fifth Intern. Symp. on Stratified Flows* Vol. 2 (Eds G A Lawrence, R Pieters, N Yonemitsu) (Vancouver: Univ. of British Columbia, 2000) p. 1035
28. Orr M H, Mignerey P C *J. Geophys. Res.* **108** 3064 (2003)
29. Serebryanyi A N, Pao K *Dokl. Phys.* (2005) (in press)
30. Serebryany A N *Dynamics Atm. Oceans* **23** 393 (1996)

PACS numbers: **43.25.+y**, **43.40.+s**, **62.60.+v**
DOI: 10.1070/PU2006v049n01ABEH005879

Parametrically phase-conjugate waves: applications in nonlinear acoustic imaging and diagnostics

V L Preobrazhenskii

1. Introduction

Wave phase conjugation (WPC) is typically understood as a wave process whose time development is the reverse of an arbitrarily specified incident wave. The interest in acoustic WPC stems from the ability of phase-conjugate waves (PCWs) to automatically focus onto objects that scatter the incident wave and to compensate the phase distortions of wave propagation in heterogeneous refractive media. Various applications of these properties for ultrasonic diagnostics, therapy, surgery, nondestructive evaluation, and underwater communications have recently been intensely discussed.

Comprehensive research of physical principles and mechanisms underlying the ultrasonic WPC began more than 20 years ago and was stimulated considerably by the results in the nonlinear optics for WPC of light. Since the early 1980s, the mainstream objective of several years of research has been to find adequate approaches to the problem of generation of ultrasonic PCWs in various condensed media. The systematized results of this research are reviewed in [1, 2].

The most promising techniques of acoustic PCWs, including phase conjugation of ultrasonic waves in parametrically active solid media such as piezoelectrics and magnetics [3 – 6] and time reversal of the acoustic signals in receiving and transmitting multichannel electronics [7, 8], appeared in the late 1980s – early 1990s. WPC techniques based on time reversal in waveguides and cavities with multiple reflection are being intensely developed [9, 10]. The supercritical parametric phase conjugation of magnetoelastic waves in magnetostrictive ceramics [2, 4, 11] is an effective way to produce PCWs with frequencies from several megahertz to several dozen megahertz for applications in medicine and defectoscopy. The fairly strong coupling between elastic and magnetic subsystems of spinel ferrite-based ceramics allows an effective modulation of the speed of sound by a high-frequency magnetic field. The modulation depth may then considerably exceed the threshold of parametric instability for the longwave phonons at room temperature. Under the conditions of supercritical pumping, a parametrically active element works as a source of stimulated phase-conjugate phonon pairs providing the giant (over 80 dB) amplification of the PCW compared with the incident wave. The ceramic technology allows manufacturing active elements of a wide variety of shapes and sizes according to the requirements of specific applications.

A numerically modeled animation of supercritical amplification in an active medium taken from [12] is available in Supplement 1 to the on-line version of this report.

The possible uses of magnetoacoustic PCW methods to autofocus ultrasound in liquid and solid matter and to autotarget ultrasonic beams to sound-scattering objects in liquids have been demonstrated in a set of experiments (reviewed in [2]). A stroboscopic visualization of autotargeting of ultrasound to air bubbles rising in water [13] is given in Supplement 2 to the on-line version of this report. The use of parametric WPC to compensate the phase aberrations in linear ultrasonic imaging is shown in [14, 15].

The combination of phase conjugation with giant conjugate-to-incident wave amplification is especially interesting for research and applications of WPC in nonlinear acoustics. Whereas the experimental and applied research on linear acoustic PCWs have been actively developing since the late 1980s (see [2, 16]), the nonlinear acoustics of PCWs became a promising field of acoustics a relatively short time ago. The nonlinear acoustics was pioneered in works [17, 18], where nonlinear distortions of wave profiles of parametrically PCWs and retrofocusing of reversed waves in homogeneous nonlinear media were studied experimentally and theoretically. Some results of research on the properties of nonlinear ultrasonic PCW beams and some potential uses of these properties for acoustic imaging are reviewed in [19].

As in optics, WPC in acoustics is a manifestation of the wave-field invariance under time reversal. Under strongly nonlinear conditions, the reversibility of wave processes is usually not ensured, resulting in the specific features of WPC in nonlinear acoustics. In this report, we discuss the physical mechanisms of retrofocusing of ultrasonic PCW beams in nonlinear and heterogeneous acoustic media. The results of the research on retrofocusing under the conditions of giant parametric amplification of PCWs and the phase conjugation of selected harmonics of the incident nonlinear wave are presented [20 – 23]. The applications of the effects of nonlinear retrofocusing are exemplified by compensation of the phase aberrations in nonlinear acoustic imaging [24, 25]. The potential applications of WPC-based autoconfocal systems for ultrasonic diagnostics of nonlinear inclusions are discussed. We consider the physical principles of the ultrasonic velocimetry based on the interaction of PCWs in the presence of moving scatterers [27]. We give examples of ultrasonic WPC used for the diagnostics of flows in liquid [27, 28].

2. Nonlinearly propagating ultrasonic PCW beams and time reversal

As noted above, the specificity of the WPC problem in nonlinear acoustics is that the propagation of the incident and the phase-conjugate waves is no longer a reversible process. The medium nonlinearity does not by itself violate the field invariance under time reversal, but may result in a considerable acceleration of irreversible dissipative processes. An example of this situation typical for acoustics is the shock distortions of the wave profile formed during the cascade generation of harmonics in a nonlinear medium [18, 29]. The amplification during the generation of the PCW emitted into a nonlinear medium is obviously dependent on the violation of the reversability of the wave process. Finally, the bandwidth of real acoustic WPC systems is usually considerably limited, resulting in a trimmed reproduction of the spectrum of nonlinear waves. Nevertheless, the first experimental and theoretical research data on nonlinear acoustic PCWs [18, 24, 25] have shown that in dispersion-free nonlinear acoustic systems, contrary to nonlinear optics, a partial violation of the field invariance under time reversal does not hinder observation and the use of the effects such as PCW autofocusing and the compensation of phase aberrations caused by inhomogeneous refraction.

3. Retrofocusing of nonlinear PCW beams in a heterogeneous medium

Typical results of the observed retrofocusing of a nonlinear PCW after passage through an aberrating layer are given in Fig. 1 [20]. Figure 1a shows the focal distribution of the sound amplitude broken by the aberrating layer. Figure 1b demonstrates how the focal acoustic field distribution is restored by the parametric PCW. The focal amplitude distribution of selected harmonics of the nonlinear PCW after passage through the aberrating layer is shown in Fig. 3c. As shown in [24, 30], the presented experimental results are due to the spatial and temporal synchronization of the harmonic's phases during their cascade generation in a dispersion-free medium. The harmonic phase synchronization concept was further developed when the selective phase conjugation of separate harmonics of nonlinear waves was studied [22, 23, 25]. These theoretical and experimental studies showed that nonlinear wave spectrum trimming by the narrow-band phase

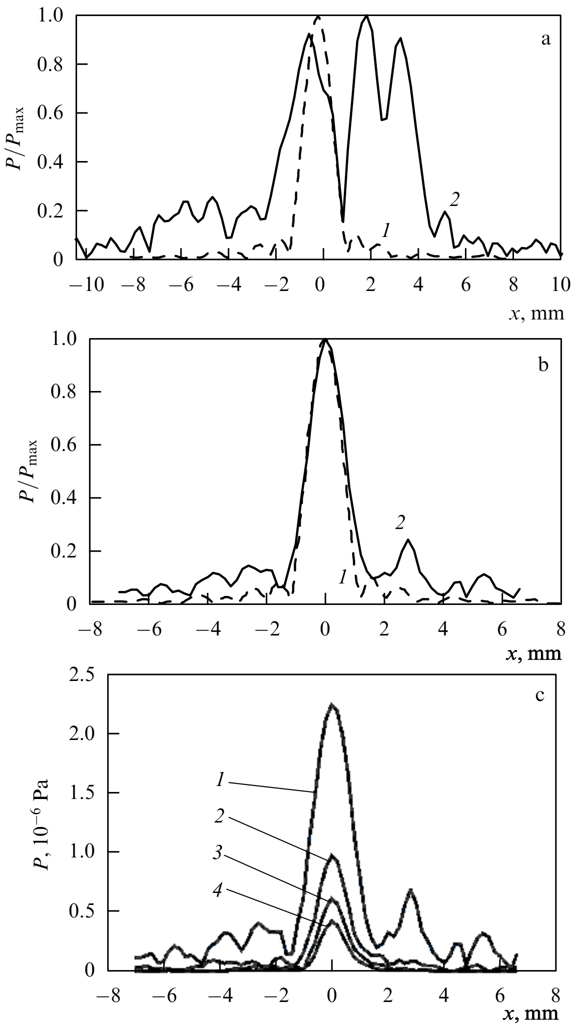

Figure 1. The focal distributions of pressures for the incident and conjugate waves (x is the distance from the axis): (a) for the incident wave without (curve *1*) and with (curve *2*) the aberrating layer; (b) normalized average pressure; curve *1* — for the incident wave without the aberrating layer and curve *2* — for the conjugate wave with the aberrating layer; (c) the amplitudes of the first four harmonics of the conjugate wave with the aberrating layer (the fundamental frequency is 10 MHz) [20].

conjugation of the second harmonic of the incident wave does not hinder the retrofocusing of finite-amplitude PCWs in a heterogeneous nonlinear medium.

4. Principles of nonlinear WPC-based acoustic imaging and diagnostics

The studies of nonlinear WPC phenomena are stimulated by a current trend to use nonlinear acoustic techniques not only for natural applications of high-intensity ultrasound such as lithotripsy, hyperthermia, and ultrasonic technology but also in traditional fields of linear acoustics such as ultrasonic diagnostics and nondestructive evaluation. 'Harmonic imaging' is a rapidly developing field of modern acoustic imaging. It is based on the analysis of harmonics generated by waves of finite amplitudes in the acoustic media in question. The techniques of harmonic imaging can be divided into two main groups. In the first group, the nonlinearity of the medium analyzed is used to form the incident acoustic beam. It should be noted that almost 30 years ago, the second harmonic was proposed to be used for the higher resolution of the acoustic microscope [31]. The number of applications of harmonic imaging for ultrasonic diagnostics is currently growing [32–34]. When focussed ultrasonic beams propagate in a nonlinear medium, the focal distribution of the second and higher harmonics of the nonlinear wave is narrower than that of the fundamental harmonics and its side lobes are lower. Besides, the generation of harmonics during wave passage through a thick medium reduces the noise originating from the refractions of the incident wave at the boundaries of the area in question. Taken together, all of the above allows considerably increasing the resolution of ultrasonic diagnostic equipment.

In the second group of harmonic imaging methods, the nonlinear response to acoustic treatment is used to obtain information about the nonlinear parameters of the medium in question and the variations of these parameters due to general or local structural changes (see [35–39]). Microcracks in a solid matter lead to the so-called contact nonlinearity, which in turn results in the anomalously amplified nonlinear acoustic response and in the more effective interactions of waves of different frequencies [36, 37]. The special nonlinear properties of solid media are used for the nondestructive evaluation of the materials. The possibilities of diagnostics using changes in nonlinear acoustic properties of biological tissues concurrent with the pathological changes in them are being discussed [40].

The possibility of the giant amplification of PCWs in the supercritical parametric mode permitted the natural expansion of the WPC technique to nonlinear acoustic imaging. The WPC technique has been combined with harmonic imaging in [24, 25]. The use of parametric PCWs for the compensation of the phase aberrations of an acoustic microscope that uses the second harmonic of the conjugate wave to view the object is shown in Fig. 2. The introduction of the aberrating layer to the confocal transmission microscope completely destroyed the image, whereas the use of WPC allowed not only restoring the image produced by the fundamental frequency of the incident beam but also obtaining a higher-resolution image produced by the second harmonic. Given in Fig. 3 are the images obtained by an acoustic microscope in which the second harmonic of the incident beam was selectively phase-conjugated [25]. The

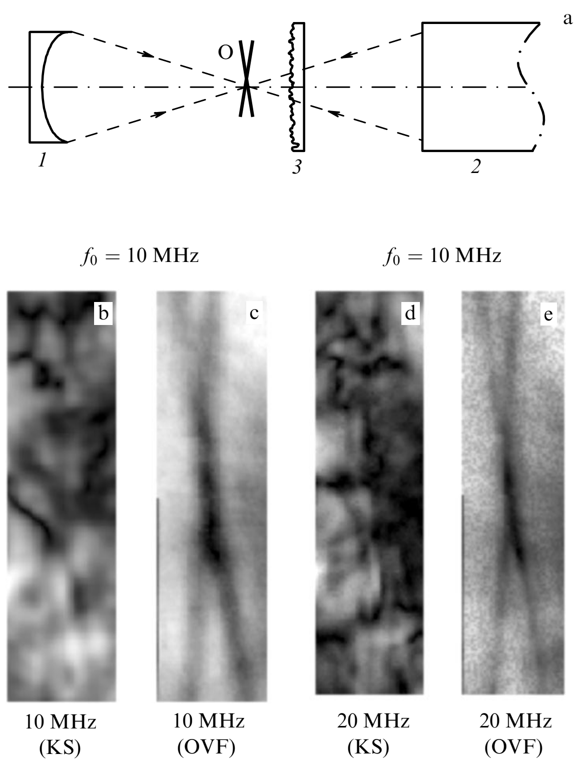

Figure 2. Acoustic images of an object restored by the phase conjugation of the fundamental harmonic of the incident wave: (a) the experimental setup (O is the object, *1* — sound transceiver, *2* — magnetoacoustic PCW amplifier, *3* — aberrating layer; (b, d) confocal microscope (CM) images produced by the fundamental and the second harmonics of the incident wave; (c, e) restored images produced by WPC [25].

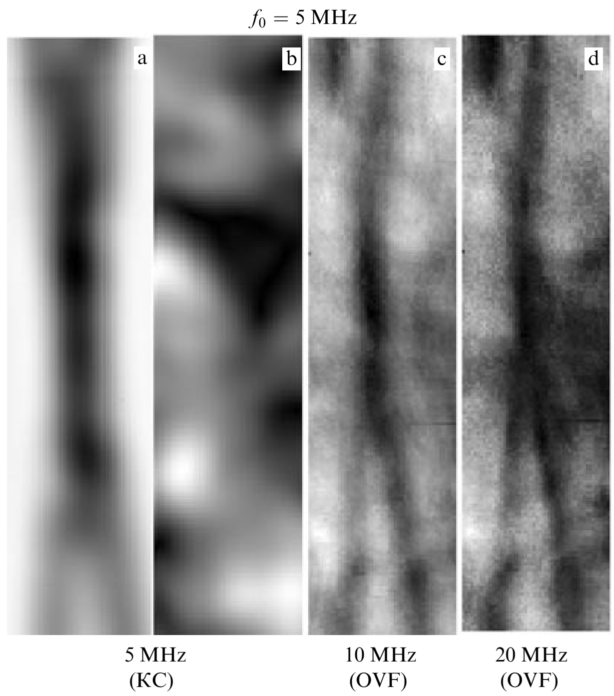

Figure 3. Acoustic confocal images produced by the fundamental harmonic at 5 MHz without (a) and with (b) an aberrating layer. (c, d) Images produced by the phase conjugation of the second harmonic of the incident wave with an aberrating layer at the frequencies 10 MHz and 20 MHz [25].

images are produced with and without an aberrating layer by the fundamental harmonic of the incident wave and by the fundamental and the second harmonics of the conjugate wave. The use of selective phase conjugation of the separate harmonic of the incident wave allows not only compensating the phase aberrations but also considerably increasing the frequency of analysis in the lower order of nonlinearity. The selective phase conjugation of harmonics also permits autofocusing ultrasound onto localized strongly nonlinear objects, which may be used for diagnostic purposes.

The PCW principle can automatically ensure that the acoustic systems are confocal. That, together with the feasibility of compensating for the phase aberrations, is useful for the nonlinear diagnostics of inclusions that are difficult to detect by linear acoustic imaging techniques. A feature of the second harmonic generation in confocal systems, caused by a phase jump of nonlinear sources in the focal plane, allows locally diagnosing the distribution of the nonlinear parameter by the second harmonic of the incident wave [41, 42]. The possibility of obtaining the image of a local inclusion produced by the second harmonic of the focussed PCW is considered in [26]. The geometry of the system and the calculated ration between the amplitude of the second harmonic registered by the sound transceiver and the position of the inclusion in the focal area are given in Fig. 4. Even small inclusions are predicted to generate a second harmonic exceeding the noise as much as the nonlinear parameters of the inclusion exceed those of the acoustic medium surrounding it.

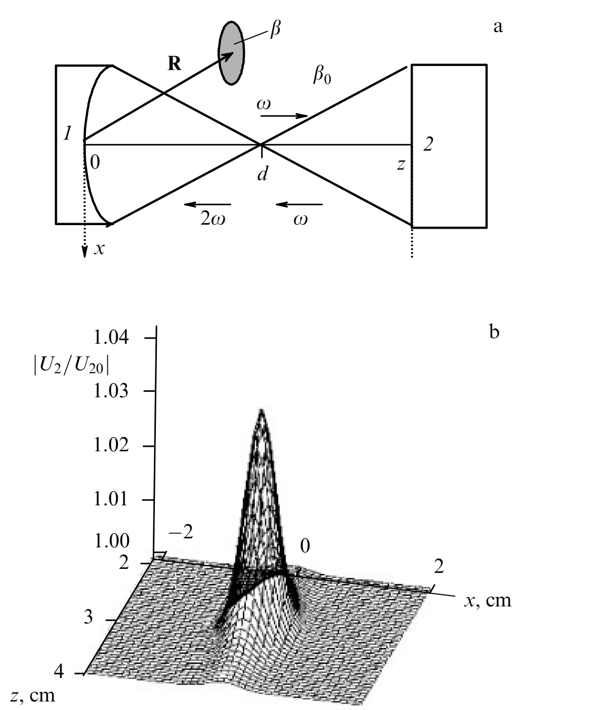

Figure 4. Acoustic imaging of inclusions using the second harmonic of a PCW: (a) the geometry of the experiment (*1* — transceiver, *2* — PCW amplifier, β and β_0 are the nonlinear parameters of the inclusion and the surrounding optical medium, respectively); (b) the response of the second harmonic, given as signal/noise ratio, to a change in position of a spherical inclusion 3 mm in diameter relative to the focus (the experimental parameters are $\omega/2\pi = 10$ MHz, $(\beta - \beta_0)/\beta_0 = 0.1$, $s = 30$ mm, and the transceiver aperture is 15 mm) [26].

5. Applications of WPC for velocity measurements and diagnostics of flows

The possible application of ultrasonic WPC that are targets themselves to a scatterer for measuring the scatterer velocity is demonstrated in [27, 43]. When PCWs of similar frequencies collided near a scatterer in experiments [44, 45], they produced ultrasound of a low difference frequency, with its phase being anomalously sensitive to the displacements of the scatterer. The movement of the scatterer was accompanied by a Doppler frequency shift of the low-frequency wave. Unlike the regular Doppler shift, which is proportional to the carrier frequency, the registered shift was proportional to the doubled frequency of one of the high-frequency waves propagating toward the receiver of the low-frequency sound. The effect is due to phase additions of the conjugate waves when the difference frequency sound wave is produced. A possible application of this effect for measuring the scatterer velocities ranging widely from 0.05 mm s^{-1} to 300 mm s^{-1} at the difference frequency of 1 MHz is demonstrated in [27, 43]. Here, the registered Doppler shift exceeded the regular values of the Doppler shift by an order of magnitude at the given frequency and the velocity of the scatterer.

The PCW principle assumes that the phase of the wave at the source is restored irrespective of the phase shifts in the forward and the reverse directions. The phase is restored in both homogeneous and heterogeneous refractive media. Flows in the medium disturb the wave invariance under time reversal and thus result in a phase shift of the conjugate wave at the transceiver. A phenomenon of this nature observed earlier was the wave front distortions that accumulated during the repeated passage of conjugate waves through a vortex in a fluid [46]. In [27, 28], a beam passing through a flow was scanned, and the PCW phase shifts were analyzed in order to obtain the images of the velocity distribution of the water flows of various geometries. The authors of [28] analyzed not only the phases of the fundamental harmonic of PCWs but also the phases of the second harmonic and of the low difference frequency signals produced by the interaction of the phase-conjugate waves of close frequencies. The experimental setup and the visualized water flow from [28] are given in Fig. 5. In this experiment, a low-frequency wave was generated by the interaction of the 20 MHz second harmonic of the conjugate wave with an additional 19 MHz pulse in the same direction, and the phase of the low-frequency wave was analyzed to produce the image. The use of the second harmonic doubled the registered phase shift, and the acoustic frequency subtraction increased the signal/noise ratio for digital processing of the registered signals by more than an order of magnitude.

6. Conclusion

The results presented here show the effectiveness of the supercritical ultrasonic WPC technique for applications in nonlinear acoustics. In heterogeneous refractive media, the waves are no longer reversible due to the conjugate wave amplification and WPC spectrum trimming. The experimental and theoretical demonstrations of the refocusing of ultrasound in such media are paving the way for the development of new techniques in acoustic imaging and diagnostics. The physical principles of these techniques are to some extent exemplified by harmonic imaging, nonlinear ultrasonic velocity measuring, and the diagnostics of flows. It

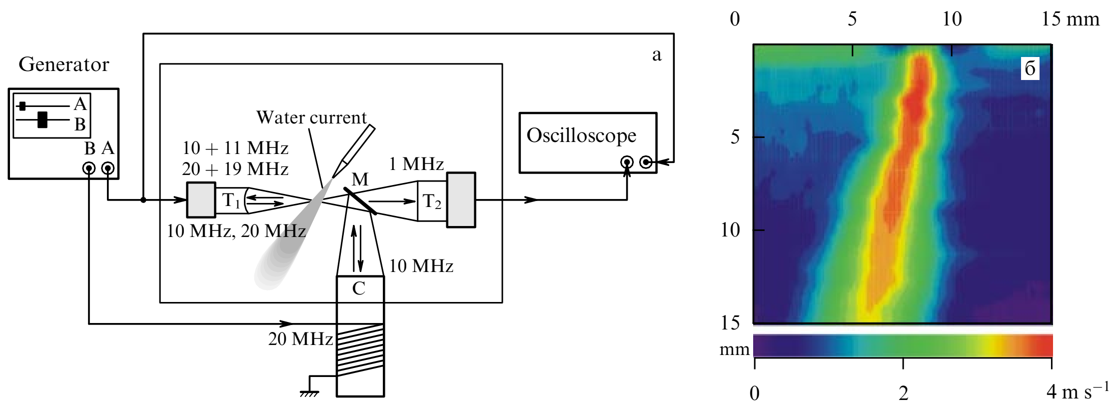

Figure 5. The PCW diagnostics of water flows: (a) the experimental setup (T1 and T2 are the ultrasound source and detector, respectively, C is the PCW amplifier, M is the deflecting plate); (b) an acoustic image of the velocity distribution in a flow [28].

would not be an overestimation to say that nonlinear WPC acoustics has recently become one of the hottest fields in physical acoustics and ultrasonics. The fundamental contribution to this field and to WPC acoustics in general made by the Russian Academy of Sciences is remarkable.

In conclusion, the author thanks F V Bunkin for the initiation and for his constant support in the work on WPC acoustics and the colleagues from the the Joint Russian – French European Laboratory of Nonlinear Magnetoacoustics (LEMAC) for their fruitful collaboration.

The publication is prepared in the framework of the fundamental research program of RAS, Coherent acoustic fields and signals and the international programs ECONET 08-154YE and INTERREG-IIIa-58, and with support from the Russian Foundation for Basic Research (Grant No. 05-02-19640-NTsNIL_a), Ecole Centrale de Lille, and the French Embassy in Moscow.

References

1. Bunkin F V, Kravtsov Yu A, Lyakhov G A *Usp. Fiz. Nauk* **149** 391 (1986) [*Sov. Phys. Usp.* **29** 607 (1986)]
2. Brysev A P, Krutyanskiĭ L M, Preobrazhenskiĭ V L *Usp. Fiz. Nauk* **168** 877 (1998) [*Phys. Usp.* **41** 793 (1998)]
3. Brysev A P et al. *Akust. Zh.* **34** 986 (1988) [*Sov. Phys. Acoust.* **34** 567 (1988)]
4. Brysev A P et al. *Akust. Zh.* **34** 1120 (1988)
5. Ohno M *Appl. Phys. Lett.* **54** 1979 (1989)
6. Ohno M et al. *J. Acoust. Soc. Am.* **106** 1330 (1999)
7. Fink M, Prada C, Wu F, in *Proc. of the IEEE Ultrasonics Symp., Montreal, PQ, 1989* Vol. 2, p. 681
8. Fink M *IEEE Trans. Ultrason. Ferroelectrics Frequency Control* **39** 555 (1992)
9. Montaldo G et al. *J. Acoust. Soc. Am.* **110** 2849 (2001)
10. Sutin A, Sarvazyan A, in *Proc. of the World Congress on Ultrasonics, Paris, France, 2003* Vol. 2, p. 863
11. Brysev A P, Krutyansky L M, Preobrazhensky V L *Phys. Vibrations* **9** (1) 52 (2001)
12. Bou Matar O, Preobrazhensky V, Pernod P *J. Acoust. Soc. Am.* **118** 2880 (2005)
13. Brysev A P et al. *Pis'ma Zh. Eksp. Teor. Fiz.* **61** 454 (1995) [*JETP Lett.* **61** 464 (1995)]
14. Yamamoto K et al. *J. Acoust. Soc. Am.* **106** 1339 (1999)
15. Brysev A et al. *Appl. Phys. Lett.* **76** 3133 (2000)
16. Fink M et al. *Rep. Prog. Phys.* **63** 1933 (2000)
17. Brysev A P et al. *Akust. Zh.* **44** 738 (1998)
18. Brysev A P et al., in *Nonlinear Acoustics at the Turn of the Millennium: ISNA 15, 15th Intern. Symp. on Nonlinear Acoustics, Göttingen Germany, 1 – 4 September 1999* (AIP Conf. Proc., Vol. 524, Eds W Lauterborn, T Kurz) (Melville, NY: AIP, 2000) p. 183
19. Brysev A P et al. *Akust. Zh.* **50** 725 (2004) [*Acoust. Phys.* **50** 623 (2004)]
20. Brysev A P et al. *Pis'ma Zh. Eksp. Teor. Fiz.* **73** 434 (2001) [*JETP Lett.* **73** 389 (2001)]
21. Cunningham K B et al. *J. Acoust. Soc. Am.* **109** 2668 (2001)
22. Brysev A P et al. *Phys. Wave Phenom.* **11** 10 (2003)
23. Preobrazhensky V L, Pernod P *Phys. Wave Phenom.* **11** 63 (2003)
24. Pyl'nov Yu, Pernod P, Preobrazhensky V *Appl. Phys. Lett.* **78** 553 (2001)
25. Krutyansky L et al. *IEEE Trans. Ultrason. Ferroelectrics Frequency Control* **49** 409 (2002)
26. Preobrazhensky S V, Preobrazhensky V L, Pernod P *Phys. Wave Phenom.* **13** 24 (2005)
27. Pyl'nov Yu V, Pernod P, Preobrazhenskii V L *Akust. Zh.* **51** 105 (2005) [*Acoust. Phys.* **51** 105 (2005)]
28. Pyl'nov Yu et al., in *Proc. of the IEEE Ultrason. Symp., Rotterdam, 2005*, Abstracts, p. 535
29. Hallaj I M et al. *Ultrasonics* **38** 885 (2000)
30. Preobrazhensky V, Pernod P, in *Proc. of the 17th Intern. Congress on Acoustics, Rome, Italy, September 2 – 7, 2001* Vol. 1 *Physical Acoustics* Pt. A (Eds A Alippi et al.) (Roma: ICA, 2002) p. 26
31. Kompfner R, Lemons R A *Appl. Phys. Lett.* **28** 295 (1976)
32. Ward B, Baker A C, Humphrey V F *J. Acoust. Soc. Am.* **101** 143 (1997)
33. Averkiou M A, Roundhill D N, Powers J E, in *Proc. of the IEEE Ultrasonics Symp., 1997* Vol. 2, p. 1561
34. Averkiou M A, in *Proc. of the IEEE Ultrasonics Symp., 2000* Vol. 2, p. 1563
35. Rudenko O V *Nerazrushayushchii Kontrol* **29** 583 (1993)
36. Solodov I Yu *Ultrasonics* **36** 383 (1998)
37. Zeng Y, Maev R G, Solodov I Yu *Can. J. Phys.* **77** 927 (1999)
38. Van Den Abeele K E-A, Johnson P A, Sutin A *Res. Nondestr. Eval.* **12** 17 (2000)
39. Van Den Abeele K E-A et al. *Res. Nondestr. Eval.* **12** 31 (2000)
40. Vignon F et al., in *Proc. of the IEEE Ultrason. Symp., Rotterdam, 2005*, Abstracts, p. 360
41. Lucas B G, Muir T G *J. Acoust. Soc. Am.* **74** 1522 (1983)
42. Kim B C , Saito S *J. Acoust. Soc. Jpn.* (*E*) **10** 143 (1989)
43. Pyl'nov Yu, Preobrazhensky V, in *Proc. of the IEEE Ultrasonics Symp., Montreal, 2004* Vol. 3, p. 1612
44. Pylnov Y, Pernod P, Preobrazhensky V *Acta Acust. Acust.* **89** 942 (2003)
45. Pyl'nov Yu, Pernod P, Preobrazhensky V, in *Proc. of the IEEE Ultrasonics. Symp., 2001* Vol. 1, p. 397
46. Roux P,Fink M, in *Proc. of the 4th French Congr. on Acoustics* Vol.1 (Marseilles: Teknea 1997) p. 951